X-ray reflection from rough layered systems

V. Holý, J. Kuběna, and I. Ohlídal

Department of Solid State Physics, Faculty of Science, Masaryk University, Kotlářská 2, 611 37 Brno, Czech Republic

K. Lischka and W. Plotz

Institute of Optoelectronics, Kepler University, Altenbergerstrasse 69, 4040 Linz, Austria

(Received 15 September 1992)

The specular and nonspecular x-ray reflectivity of a rough multilayer is calculated on the basis of the distorted-wave Born approximation. The theory explains the existence of maxima in the angular distribution of a nonspecularly reflected wave. The interface roughness has been characterized by root-mean-square roughness, lateral correlation length, and the fractal dimension of the interface. It has been demonstrated that these parameters can be obtained from nonspecular reflectivity measurements. Calculations based on this theory compare well with data measured on rough layered samples.

I. INTRODUCTION

X-ray specular reflectivity measurement is a powerful method for investigating surfaces and multilayers. Experimental reflectivity curves can be analyzed using formulas following from the Fresnel formalism of optical reflection and refraction[1] in a multilayer with smooth interfaces. This approach can yield thicknesses and refractive indices of individual layers.

In order to study the quality of interfaces in a multilayer (interface roughness) a more sophisticated description of the reflection process should be applied. In a series of papers[2-7] the influence of the interface roughness on the Fresnel reflection amplitude has been assumed in the form of a multiplication term analogous to the static Debye-Waller factor known from the x-ray diffraction. Two different forms of this term are used in the literature. The first one[2] can be derived by averaging all the phase terms in the reflectivity of a multilayer with smooth interfaces over random layer thicknesses. This averaging is not legitimate from a general viewpoint of statistics; the final formulas, however, agree with experimental results quite well and they only fail for small incidence angles.[4] A modified form of the roughness term has been found on the basis of general scattering theory[4-7] that fits the experimental data for all incidence angles.

The specular wave reflected from a rough multilayer represents the coherent component of the entire reflected wave. This component can be described using the coherent approximation of the reflection process, which only includes the point properties of the rough interface, i.e., on its mean-square roughness. In order to investigate the in-plane correlation in a rough interface a measurement of the incoherent component of the reflected wave is necessary. The incoherent contribution to the reflected wave is represented by the nonspecular (diffuse) wave. The angular distribution of the intensity reflected nonspecularly from a rough surface has been measured and intensity maxima have been observed if the incidence an-gle and/or the angle between the surface and the diffuse wave (the exit angle) equals the critical angle θ_c of total x-ray reflection.[8-10] These maxima are known as "Yoneda peaks." Similar results have been obtained for rough multilayers.[2,11]

Theoretical description of the nonspecular reflection on a single rough surface has been developed[12] using the Born approximation (BA) and the distorted-wave Born approximation (DWBA) known from the general scattering theory.[13,14] In the Born approximation the reflection process is considered as a scattering from independent scatterers (electrons) being irradiated by an incident plane wave. Within this approach the differential cross section is calculated for the scattering from the incident plane wave $|\psi_1\rangle$ into the final plane wave $|\psi_2\rangle$. The essence of DWBA consists in the assumption that the undisturbed states $|\psi_1\rangle$ and $|\psi_2\rangle$ correspond to two different wave fields in an ideal system (i.e., with smooth surface). Then, the surface roughness acts as a disturbance and it causes the scattering from $|\psi_1\rangle$ into $|\psi_2\rangle$.

It has been demonstrated by numerical calculations of both coherent and incoherent waves[12] that the BA approximation is suitable for greater incidence angles, where the DWBA fails. On the other hand, for smaller angles of incidence DWBA is suitable and BA is not applicable. Below the critical angle the BA diverges, since it does not include the effect of total reflection. The formula for the specular reflectivity of a single rough surface following from the conventional formalism with the modified roughness term[4-7] coincides with that from DWBA for small incidence angles and with that from BA for greater angles. Moreover, the DWBA method succeeded in the explanation of the nature of the Yoneda peaks,[12] where the BA fails.[2,3]

The DWBA approach has been used for studying the structure of wet rough surfaces.[15] The form of the Yoneda peaks has been simulated and a good agreement with experiments has been achieved.

The aim of this paper is to generalize the DWBA ap-

proach for the case of a layered system with rough interfaces. We find explicit formulas for coherent reflectivity and differential cross section of the nonspecular scattering for a multilayer with rough interfaces and demonstrate that the angular distribution of the nonspecular component is closely connected with the specular reflectivity and with the fractal properties of the rough interfaces. We show that in the case of a multilayer the positions of the peaks of this distribution can easily be explained. We compare the theoretical results with measurements performed on layered samples and obtain an estimate for the in-plane correlation length of the rough interfaces.

II. THEORY

In this section we derive the basic equation for the coherent reflectivity and the incoherent scattering cross section for x-ray reflection on a random rough multilayer. We follow the calculation procedure of the DWBA method[12] and we generalize it for the case of a multilayer.

Let us start from the wave equation

$$(\Delta + K^2)|\psi\rangle = V(\mathbf{r})|\psi\rangle. \tag{1}$$

The scattering potential V is given by

$$V(\mathbf{r}) = K^2[1 - n^2(\mathbf{r})], \tag{2}$$

where $K = 2\pi/\lambda$ is the vacuum wave-vector length and $n(\mathbf{r})$ is the refraction index of the system (assumed dependent on the position $\mathbf{r}$). We assume that the measured reflectivity signal does not depend on the actual (microscopic) shape of the interfaces, i.e., the mean correlation length of the rough interfaces is much shorter than the size of the sample irradiated area. Then, all the measured quantities are averaged over the statistical ensemble of all microscopic configurations of the interface profiles.

The scattering potential can be split into two parts,

$$V(\mathbf{r}) = V^{(0)}(\mathbf{r}) + V^{(1)}(\mathbf{r}),$$

where $V^{(0)}$ represents the undisturbed system and $V^{(1)}$ is the perturbance due to the interface roughness. Within the DWBA approximation[12,13] the averaged differential cross section of the light scattering from a random system can be expressed as

$$\frac{d\sigma}{d\Omega} = \frac{\langle|V_{12}|^2\rangle}{16\pi^2}, \tag{3}$$

where $V_{12} = V_{12}^{(0)} + V_{12}^{(1)}$, $V_{12}^{(0)} = \langle\psi_2|V^{(0)}|\phi_1\rangle$ is the scatering matrix element of the undisturbed system, and $V_{12}^{(1)} = \langle\psi_2|V^{(1)}|\psi_1\rangle$ is that of the perturbation. $|\psi_1\rangle$ and $|\psi_2\rangle$ are two independent eigenstates of the undisturbed system,

$$|\phi_1\rangle = \exp(i\mathbf{K}^{\text{inc}} \cdot \mathbf{r})$$

describes the incident plane wave.

The differential cross section (3) is proportional to the probability of scattering from the state $|\psi_1\rangle$ into $|\psi_2\rangle$ The intensity of the waves scattered into a small solid angle $d\Omega$ is then

$$dI = I_{\text{inc}}\frac{d\sigma}{d\Omega}\,d\Omega, \tag{4}$$

where I_{inc} is the flux density of the primary wave given in counts per area per time.

The undisturbed system is represented by a multilayer with ideally smooth interfaces (see Fig. 1). The jth layer lies between the $(j-1)$th and the jth interfaces, its thickness is d_j, and refractive index n_j. The layer $j = N$ lies at the substrate, $n_1 = 1$ is the vacuum refractive index, and n_{N+1} is the refractive index of the substrate. Similarly to the case of a single rough surface[12] we choose the following undisturbed states:

$$\begin{aligned}
\psi_1(\mathbf{r}) &= T_1(z)\exp[i\mathbf{K}_1(z)\cdot\mathbf{r}] \\
&\quad + R_1(z)\exp[i\mathbf{K'}_1(z)\cdot\mathbf{r}],
\end{aligned} \tag{5}$$

$$\begin{aligned}
\psi_2(\mathbf{r}) &= T_2^*(z)\exp[i\mathbf{K}_2^*(z)\cdot\mathbf{r}] \\
&\quad + R_2^*(z)\exp[i\mathbf{K'}_2^*(z)\cdot\mathbf{r}].
\end{aligned}$$

$R_{1,2}$ and $T_{1,2}$ are the complex amplitudes of the transmitted and the reflected beams, respectively, for the states 1 and 2. $\mathbf{K}_{1,2}$ and $\mathbf{K'}_{1,2}$ are their wave vectors. For an ideal multilayer system $R_{1,2}$, $T_{1,2}$, $\mathbf{K}_{1,2}$, and $\mathbf{K'}_{1,2}$ only depend on the coordinate z perpendicular to the interfaces and they can be obtained using conventional x-ray optics.[1] The z axis is introduced according to Fig. 1, and z_j is the z coordinate of the jth interface ($z_1 = 0$). The eigenstate $|\psi_2\rangle$ is chosen so that it represents a time-inverted state; the amplitude of the wave emitted by the multilayer in the eigenstate $|\psi_2\rangle$ is therefore $T_2(0)$. The angle of incidence of the primary wave $|\psi_1\rangle$ is θ_1; the exit angle (i.e., the angle between the free surface and the emitted wave $|\psi_2\rangle$) is θ_2.

The matrix element $V_{12}^{(0)}$ of the undisturbed system can be calculated directly. It is connected with the reflectivity $\mathcal{R}$ of the ideal system by the formula[12]

$$|V_{12}^{(0)}|^2 = SK^2\sin^2(\theta_1)\,\mathcal{R}\,\delta(\mathbf{K}_{2\|} - \mathbf{K}_{1\|}), \tag{6}$$

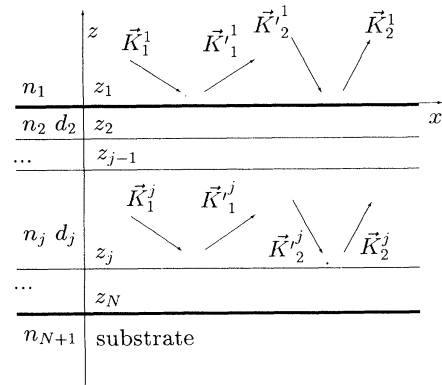where the vector components parallel to the interface are

FIG. 1. Sketch of an ideal multilayer with undisturbed states $|\psi_1\rangle$ and $|\psi_2\rangle$.

denoted by $\|$. This expression is valid if we assume the irradiated surface area S is large enough and the Dirac deltas in (6) express the specular nature of the scattering from an ideal layer system ($\theta_1 = \theta_2$).

Now, let us consider a system with rough interfaces. The actual profile of the jth interface is described by a random displacement $u_j(x, y)$ (see Fig. 2), where the coordinates x, y are perpendicular to z, and the x axis lies in the plane of incidence. We make a natural assumption that each layer has always a nonzero thickness, i.e., the neighboring interfaces do not intersect. The perturbation Hamiltonian $V^{(1)}(\mathbf{r})$ is then given by

$$V^{(1)}(\mathbf{r}) = K^2 \sum_{j=1}^{N} (n_j^2 - n_{j+1}^2) P_j(\mathbf{r}), \tag{7}$$

where $P_j(\mathbf{r})$ is a random shape function of the jth interface defined as follows:

$$P_j(\mathbf{r}) = \begin{cases} 1, & z \in \langle z_j, z_j + u_j(x, y) \rangle \text{ for } u_j(x, y) > 0 \\ -1, & z \in \langle z_j + u_j(x, y), z_j \rangle \text{ for } u_j(x, y) < 0 \\ 0 & \text{elsewhere.} \end{cases} \tag{8}$$
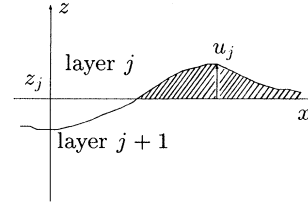

FIG. 2. Schematic of a rough interface between the jth and the $(j+1)$th layers.

Let us denote $S_\pm^j$ the part of the jth interface where $u_j(x, y) > 0$ or < 0. We introduce the random functions

$$F_\pm^j(\mathbf{q}) = \int_{S_\pm^j} dx\, dy \int_{z_j}^{z_j + u_j(x, y)} dz\, \exp(-i\mathbf{q} \cdot \mathbf{r})$$

and denote $T_{1,2}^j$, $R_{1,2}^j$, $\mathbf{K}_{1,2}^j$, and $\mathbf{K}_{1,2}'^j$ the values of functions $T, R, \mathbf{K}$, and $\mathbf{K}'$ in the jth layer ($\mathbf{K}^{\mathrm{inc}} = \mathbf{K}_1^1$).

The matrix element of the perturbation Hamiltonian can be written as follows:

$$V_{12}^{(1)} = \langle \psi_2 | V^{(1)} | \psi_1 \rangle = K^2 \sum_{j=1}^{N} (n_j^2 - n_{j+1}^2)\, [\, T_1^j T_2^j F_+^j(\mathbf{q}_0^{\,j}) + T_2^j R_1^j F_+^j(\mathbf{q}_2^{\,j}) + R_2^j T_1^j F_+^j(\mathbf{q}_1^{\,j}) + R_1^j R_2^j F_+^j(\mathbf{q}_3^{\,j})$$

$$+ T_1^{j+1} T_2^{j+1} F_-^j(\mathbf{q}_0^{\,j+1}) + T_2^{j+1} R_1^{j+1} F_-^j(\mathbf{q}_2^{\,j+1}) + T_1^{j+1} R_2^{j+1} F_-^j(\mathbf{q}_1^{\,j+1})$$

$$+ R_1^{j+1} R_2^{j+1} F_-^j(\mathbf{q}_3^{\,j+1}) \,], \tag{9}$$

where we have denoted

$$\mathbf{q}_0^{\,j} = \mathbf{K}_2^j - \mathbf{K}_1^j, \quad \mathbf{q}_1^{\,j} = \mathbf{K}'_2^j - \mathbf{K}_1^j,$$

$$\mathbf{q}_2^{\,j} = \mathbf{K}_2^j - \mathbf{K}'_1^j, \quad \mathbf{q}_3^{\,j} = \mathbf{K}'_2^j - \mathbf{K}'_1^j.$$

A. The specular (coherent) reflectivity

The differential cross section (3) can be split into the coherent (specular) and the incoherent (nonspecular, diffuse) parts

$$\frac{d\sigma}{d\Omega} = \left(\frac{d\sigma}{d\Omega}\right)_C + \left(\frac{d\sigma}{d\Omega}\right)_I$$

$$= \frac{1}{16\pi^2} |V_{12}^{(0)} + \langle V_{12}^{(1)} \rangle|^2$$

$$+ \frac{1}{16\pi^2} [\langle |V_{12}^{(1)}|^2 \rangle - |\langle V_{12}^{(1)} \rangle|^2]. \tag{10}$$

The coherent part of the scattered wave represents the specular scattering from $|\psi_1\rangle$ into $|\psi_2\rangle$. Thus $\mathbf{K}_1^j = \mathbf{K}'_2^j$ and $\mathbf{K}'_1^j = \mathbf{K}_2^j$ and, therefore, $\mathbf{q}_1^{\,j} = \mathbf{q}_2^{\,j} = 0$, $\mathbf{q}_3^{\,j} = -\mathbf{q}_0^{\,j}$. Calculating the average $\langle V_{12}^{(1)} \rangle$ we have to calculate the averages $\langle F_\pm^j(\mathbf{q}) \rangle$ and $\langle F_\pm^j(0) \rangle$. In this calculation we assume that the random shifts $u_j(x, y)$ represent a stationary random process with the probability density

$p_j(u)$ and zero mean. The random functions $u_j(x, y)$ and $u_l(x, y)$ are not correlated if $j \neq l$.

If the area S is large enough, the surface integrals $\int_S dx\, dy$ occurring in these averages can be approximated by the Kronecker deltas and after some algebra we get[12]

$$\langle F_\pm^j(0) \rangle = S\delta_{q_x,0}\delta_{q_y,0}\mu_\pm^j,$$

$$\langle F_\pm^j(\mathbf{q}) \rangle = \frac{i}{q_z} S\delta_{q_x,0}\delta_{q_y,0} U_\pm^j(q_z), \tag{11}$$

where

$$\mu_\pm^j = \int_{-\infty}^{\infty} du\, p_j(u)\, u Y(\pm u),$$

$$U_\pm(q_z) = -\tfrac{1}{2} + \int_{-\infty}^{\infty} du\, p_j(u) \exp(-iq_z u) Y(\pm u),$$

and $Y(x)$ is the Heaviside function [$Y(x) = 1$ for $x \geq 0$ and $Y(x) = 0$ for $x < 0$]. In the following we will assume that the probability density is a symmetric function. Then, $\mu_+^j = \mu_-^j = \mu^j$. Setting Eq. (11) into (9), we obtain an explicit formula for $\langle V_{12}^{(1)} \rangle$. Comparing this expression with (6), we find that in the coherent approximation the perturbation yields an additional term to the ideal reflectivity. For the coherent reflectivity amplitude of a rough multilayer system we obtain finally

$$R_C = R_1^1 + \frac{K^2}{q_z^1} \sum_{j=1}^{N} (n_j^2 - n_{j+1}^2)(\{(T_1^j)^2 U_+^j(q_z^j) - (R_1^j)^2 [U_+^j(q_z)]^*\}/q_z^j$$

$$+ \{(T_1^{j+1})^2 U_-^j(q_z^{j+1}) - (R_1^{j+1})^2 [U_-^j(q_z^{j+1})]^*\}/q_z^{j+1} - 2i\mu^j(T_1^j R_1^j + T_1^{j+1} R_1^{j+1})). \tag{12}$$

B. The diffuse (incoherent) scattering

Considering the diffuse scattering from a rough multilayer, both eigenstates $|\psi_1\rangle$ and $|\psi_2\rangle$ must be treated independently. According to (10) the differential cross section of the incoherent scattering is

$$\left(\frac{d\sigma}{d\Omega}\right)_I = \frac{1}{16\pi^2} \, \mathrm{Cov}(V_{12}^{(1)}, V_{12}^{(1)}), \tag{13}$$

where $\mathrm{Cov}(a,b) = \langle ab^*\rangle - \langle a\rangle\langle b\rangle^*$ is the covariance of two random quantities a and b.

Setting Eq. (9) into (13), we calculate the differential cross section. In the final formula the expressions

$$\mathrm{Cov}(F_\pm^j(\mathbf{q}_m), F_\pm^j(\mathbf{q}_n)) \tag{14}$$

occur for $\mathbf{q}_{m,n} = \mathbf{q}_{0,1,2,3}$. Similarly to the case of a single rough surface[12] this calculation can substantially be simplified assuming that the eigenstates $|\psi_{1,2}\rangle$ in the jth layer in points $\mathbf{r}$, where $z_j < z < z_j + u_j(x,y)$ (hatched regions in Fig. 2), can be replaced by those of the $(j+1)$th layer. The validity of this assumption for the case of a single surface has been discussed in Ref. 12, for the case of a multilayer, and that discussion will be presented in Sec. IV. Then, instead of (14) we have to evaluate the covariance

$$Q_{mn}^j = \mathrm{Cov}(F_+^j(\mathbf{q}_m^{j+1}) + F_-^j(\mathbf{q}_m^{j+1}), F_+^j(\mathbf{q}_n^{j+1}) + F_-^j(\mathbf{q}_n^{j+1})).$$

This covariance can easily be expressed using the statistical dispersion $\sigma_j = \sqrt{\langle u_j^2\rangle}$ of the random roughness profile [the root-mean-square (rms) roughness] and its correlation function

$$C_j(\mathbf{r} - \mathbf{r}') = \langle u_j(x,y) u_j(x',y')\rangle,$$

if both points $\mathbf{r}$ and $\mathbf{r}'$ lie at the same interface. We obtain

$$Q_{mn}^j = \frac{S}{q_{mz}^{j+1}(q_{nz}^{j+1})^*} \exp[-\sigma_j^2((q_{mz}^{j+1})^2 + (q_{nz}^{j+1})^{*2})/2]$$

$$\times \int_S dx\, dy \exp[-i(q_x x + q_y y)]\{\exp[q_{mz}^{j+1}(q_{nz}^{j+1})^* C_j(x,y)] - 1\}, \tag{15}$$

where q_x, q_y are common components of $\mathbf{q}_0^j, \mathbf{q}_1^j, \mathbf{q}_2^j$, and $\mathbf{q}_3^j$ into the smooth layer surface and we have assumed the normal distribution of random shifts u_j. The final formula for the incoherent differential cross section is

$$\left(\frac{d\sigma}{d\Omega}\right)_I = \frac{K^4}{16\pi^2} \sum_{j=1}^{N} |n_j^2 - n_{j+1}^2|^2 \{\, Q_{00}^j(|T_1^{j+1} T_2^{j+1}|^2 + |R_1^{j+1} R_2^{j+1}|^2) + Q_{11}^j(|T_2^{j+1} R_1^{j+1}|^2 + |T_1^{j+1} R_2^{j+1}|^2)$$

$$+ 2\,\mathrm{Re}[Q_{02}^j T_1^{j+1} T_2^{j+1}(R_1^{j+1} T_2^{j+1})^* + (Q_{02}^j R_1^{j+1} R_2^{j+1})^* T_1^{j+1} R_2^{j+1}$$

$$+ Q_{01}^j T_1^{j+1} T_2^{j+1}(T_1^{j+1} R_2^{j+1})^* + (Q_{01}^j R_1^{j+1} R_2^{j+1})^* R_1^{j+1} T_2^{j+1}$$

$$+ Q_{03}^j T_1^{j+1} T_2^{j+1}(R_1^{j+1} R_2^{j+1})^* + Q_{21}^j T_2^{j+1} R_1^{j+1}(T_1^{j+1} R_2^{j+1})^*]\}. \tag{16}$$

If we restrict ourselves to the case $|q_{mz}^{j+1}\sigma_j|^2 \ll 1$ after replacing the exp function in (15) by the first two terms of its Taylor series we get the simpler expression

$$\left(\frac{d\sigma}{d\Omega}\right)_I = \frac{SK^4}{16\pi^2} \sum_{j=1}^{N} |n_j^2 - n_{j+1}^2|^2 |(T_1^{j+1} T_2^{j+1} + R_1^{j+1} R_2^{j+1}) \exp[-(\sigma_j q_{0z}^{j+1})^2/2]$$

$$+ (T_1^{j+1} R_2^{j+1} + T_2^{j+1} R_1^{j+1}) \exp[-(\sigma_j q_{1z}^{j+1})^2/2]|^2 C_j(q_x, q_y). \tag{17}$$

C_j denotes a two-dimensional Fourier transform of the correlation function C_j:

$$C_j(q_x, q_y) = \int_S dx\, dy\, C_j(x, y) \exp[-i(xq_x + yq_y)].$$

Formulas (12), (16), and (17) can be used for a direct computation of the coherently and incoherently scattered intensities. For the incoherent intensity, a suitable form of the correlation function $C(x - x', y - y')$ must be chosen. We postulate the correlation function in the form resulting from the fractal description of random rough surfaces[12,16]

$$C_j(x - x', y - y') = \sigma_j^2 \exp\left[-\left(\frac{\rho}{\Lambda_j}\right)^{2h}\right], \qquad (18)$$

where $\rho = \sqrt{(x - x')^2 + (y - y')^2}$ and Λ_j is the correlation length of the jth interface. The coefficient h is connected with the fractal dimension $D_j = 3 - h$ of the jth interface.

The terms occurring on the right-hand side of Eq. (17) have a clear physical meaning; they describe several processes contributing to the diffusely scattered wave. For instance, the term

$$T_1^{j+1} T_2^{j+1} \exp[-(\sigma_j q_{0z}^{j+1})^2]$$

expresses the scattering from the transmitted wave with amplitude T_1^{j+1} into the wave with amplitude T_2^{j+1}. The change of the wave vector connected with this process is $\mathbf{q}_0^{j+1} = \mathbf{K}_2^{j+1} - \mathbf{K}_1^{j+1}$. The process corresponding to the term $T_1^{j+1} R_2^{j+1}$ is a scattering from the transmitted wave with amplitude T_1^{j+1} into the reflected wave with amplitude R_2^{j+1}. The corresponding wave vector change is then $\mathbf{q}_1^{j+1} = \mathbf{K'}_2^{j+1} - \mathbf{K}_1^{j+1}$. The physical meaning of the other terms is similar.

III. NUMERICAL AND EXPERIMENTAL EXAMPLES

In this section we will demonstrate the theoretical results by numerical calculations of nonspecular intensity reflected from layered systems and compare the theory with experiments.

The nonspecular intensity component can be measured by means of a triple-axis x-ray diffractometer, the first and second axes being connected with a crystal monochromator and the sample, respectively. On the third axis an angularly sensitive element is mounted (an analyzing crystal or a multicrystal arrangement), so that the entrance solid angle Ω_{ap} of the detector is very narrow in the incidence plane. In a simpler version the angular sensitivity of the detector in the incidence plane can be achieved by a narrow slit instead of the analyzing crystal; the slit and the detector can rotate along the rotation axis of the sample. The height of Ω_{ap} (perpendicular to the incidence plane) is only limited by the height of the detector aperture window.

Both the sample and the entrance angular aperture Ω_{ap} can be rotated independently. The angular position of the sample determines θ_1; the exit angle θ_2 is controlled by rotating Ω_{ap}.

There are two scanning modes known from the literature.[2,11] In the θ_2 mode only the analyzer rotates, so that the incidence angle θ_1 remains constant and the exit angle θ_2 is changed. In the θ_1 mode only the sample rotates, thus both the angles $\theta_{1,2}$ are changed and their sum $2\theta = \theta_1 + \theta_2$ is kept constant.

Figure 3 presents the diffuse differential cross section in the θ_1 scan calculated for a Si layer on glass for three various values of the coefficient h in Eq. (18). For $\theta_1 = \theta_c$ and $\theta_1 = 2\theta - \theta_c$ the Yoneda peaks are clearly visible, where θ_c is the critical incidence angle for the upper layer.[8–10,12] Moreover, the dependence of the nonspecular intensity on θ_1 exhibits subsidiary maxima; their forms and positions are similar to those of the dependence of the specular intensity on θ_1. A more detailed numerical analysis showed that the nonspecular component of the reflected intensity has been created mainly by the contribution of the upper interface, i.e., the terms with $j > 1$ in the sum on the right-hand side of Eq. (16) can be neglected with respect to the first term. A significant contribution of deeper interfaces to the nonspecular intensity can only be established in the case of very thin layers.

The slight asymmetry of the Yoneda peaks in Fig. 3 is caused by the dependence of the irradiated sample area S on the angle of incidence θ_1. The height of the peaks grows with growing dispersions σ_j and with growing h. The dependence of this height on the correlation lengths Λ_j is not simple; there is a maximum of the Yoneda peak height for a certain value of Λ_j.

The form of the curves in Fig. 3 substantially depends on h. For $h = 1$ there is no maximum of the nonspecular intensity near the specular peak [i.e., near the point $\theta_1 = \theta_2 = (2\theta)/2$], while for $h < 0.5$ a broad maximum appears in that region.

Figure 4 shows the θ_2 scan calculated for a periodical x-ray mirror with the structure according to Table I. The form of the curve resembles that of the coherent reflectivity $\mathcal{R}_C = |R_C|^2$, whose dependence on θ_1 is plotted in Fig. 4 by the dashed line. This behavior can easily be explained. The nonspecular component of the reflected wave is produced by the scattering of the waves represented by the ideal eigenstate $|\psi_1\rangle$ into the eigenstate $|\psi_2\rangle$. Therefore, the maximum of the nonspecular component appears if the intensities of both the eigenstates
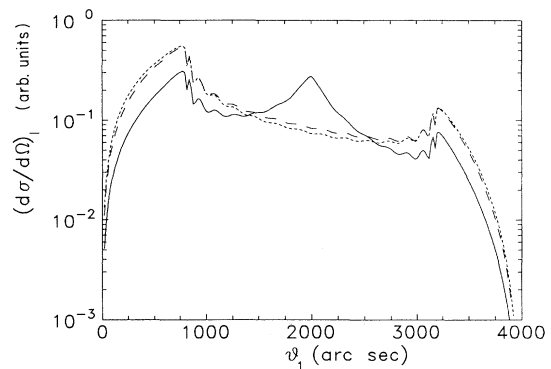

FIG. 3. Calculated diffuse differential cross sections in the θ_1 scan ($2\theta = 4000$ arc sec) for a Si layer (thickness 640 Å) on glass. The roughness parameters are $\sigma_1 = \sigma_2 = 5$ Å, $\Lambda_1 = \Lambda_2 = 1000$ Å, $h = 0.2$ (full line), 0.5 (dashed line), and 1.0 (dotted line); $\lambda = 1.54$ Å.
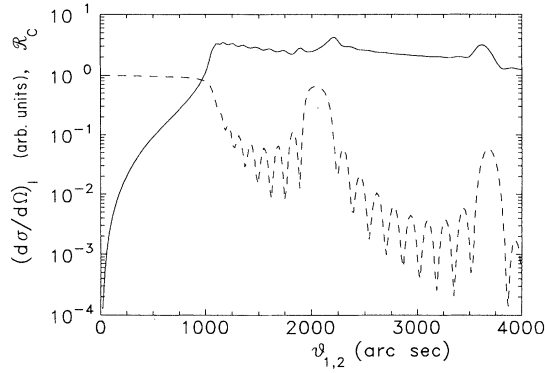
FIG. 4. Calculated diffuse differential cross section in the θ_2 scan (full line, $\theta_1 = 2000$ arc sec) and the coherent reflectivity $\mathcal{R}_C(\theta_1)$ (dashed line) of the x-ray mirror after Table I; $\lambda = 1.54$ Å.
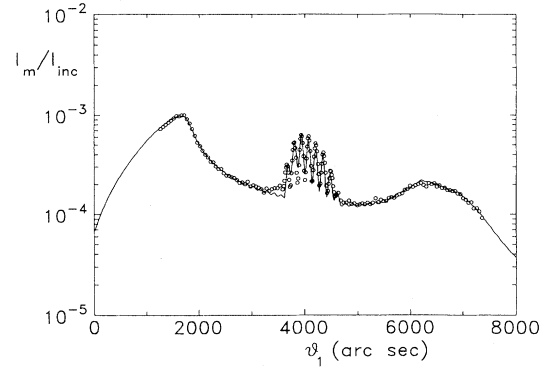

FIG. 5. Measured (circles) and calculated (line) θ_1 scan of sample A (see Tables II and III), $2\theta = 8640$ arc sec. The curve has been calculated assuming $h = 1$.

exhibit a maximum. In the θ_2 scan the angle θ_1 and the intensity of $|\psi_1\rangle$ are constant; the diffuse component only depends on the intensity of $|\psi_2\rangle$ as a function of θ_2. Therefore, a maximum of the nonspecular component appears if the intensity of the ideal wave field $|\psi_2\rangle$ (and, thus, $\mathcal{R}_C$) exhibits a maximum at the free surface. An extremely strong maximum should be observed, if both θ_1 and θ_2 equal an angular position of the maximum of the coherent reflectivity $\mathcal{R}_C(\theta_1)$. This effect has been established experimentally by Kortright.[11]

The intensity measured by the diffractometer can be expressed as

$$I_m(\theta_1, \theta_2) = I_{\text{inc}} \left[\int_{\Omega_{\text{ap}}} \left(\frac{d\sigma}{d\Omega} \right)_I d\Omega + F(\theta_1, \theta_2) \mathcal{R}_C \right],$$

where $F(\theta_1, \theta_2)$ is an instrumental function given by the convolution of the shape function of the primary beam with Ω_{ap}. The second term on the right-hand side of this formula expresses the fact that for certain values of $\theta_{1,2}$ not only the diffuse component but also a certain part of the specularly reflected wave penetrates the entrance aperture Ω_{ap}. In the θ_1 scan this effect can be observed for $\theta_1 \approx \theta_2 \approx (2\theta)/2$.

Figures 5 and 6 represent two examples of our experimental results and their numerical treatment. The experiments have been performed using the simpler version of the experimental arrangement with a narrow slit in

front of the detector rotating along the sample rotation axis. We used a conventional 2-kW Cu x-ray tube. The divergence of the primary beam has been limited by a crystal collimator, it was smaller than 20 arc sec. Two samples denoted A and B have been investigated; their structure is given in Table II. The geometrical parameters of the experimental arrangement are summarized in Table III.

Figure 5 shows the θ_1 scan of sample A; the narrow peaks near $\theta_1 = 4000$ arc sec are caused by the coherent wave; both the Yoneda peaks are clearly visible. The results of sample B (θ_1 scan) are plotted in Fig. 6.

We tried to fit the θ_1 scans of both samples with the theory assuming $h = 1$ (the full line in Fig. 5 and the dotted line in Fig. 6). In the fit procedure we used the σ_j values following from the fits of the coherent reflectivities and we found the most probable values of Λ_1 of the free surface (Table II). The theory with $h = 1$ fits the experimental results of sample A quite well, while it fails for sample B. For that sample a better coincidence was achieved assuming h free (full line in Fig. 6). The surface structure of the gold layer in sample A can be

TABLE I. The structure of the x-ray mirror. The rms roughnesses of all interfaces are $\sigma_j = 10$ Å; the lateral correlation lengths are $\Lambda_j = 1000$ Å.

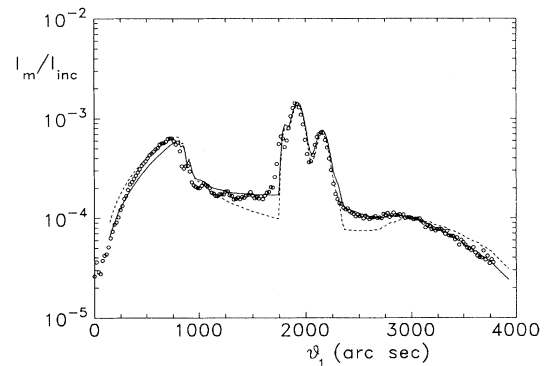| Free surface	
Si layer 65 Å	
	repeated 10 times
Mo layer 25 Å	
substrate	

FIG. 6. The same situation as in Fig. 5, sample B, $2\theta = 4030$ arc sec. In the calculations we assumed $h = 1$ (dotted line) and $h = 0.036$ (full line—the best fit with the theory).

TABLE II. Structure parameters of samples A and B from the fits of the experimental θ_1 scans. The scans are not sensitive to the roughness parameters of the layer-substrate interface. The nominal thickness values follow from the growth process; the values denoted with * have been obtained from the fit of the coherent reflectivity.

		Sample A	Sample B
Free surface	σ_1^*	(11 ± 1) Å	(14 ± 3) Å
	h	1 fixed	1 fixed
	Λ_1	(270 ± 60) Å	(1100 ± 500) Å
	h		0.36 ± 0.05
	Λ_1		(2000 ± 500) Å
Layer	material	gold	silicon
	thickness*	(1035 ± 20) Å	(640 ± 30) Å
	nominal value	1040 Å	640 Å
Substrate	material	silicon	glass

described by a Gaussian random process with Gaussian lateral correlation function ($h = 1$, the fractal dimension 2). The surface of the silicon layer in sample B is likely to be represented with a more jagged profile with higher fractal dimension ($h < 1$).[16]

IV. DISCUSSION

Deriving Eq. (16), we have replaced the actual wave field in the hatched regions of the jth layer in Fig. 2 by the wave field in the $(j+1)$th layer. Similar simplification has been performed[12] for the case of a single rough surface. The applicability of this simplification can simply be proved by calculating the diffusely scattered intensity under the opposite simplification, i.e., replacing the actual wave field in the $(j + 1)$th layer in the "valleys" by that in the jth layer. The numerical calculations proved that the difference between both intensities grows with growing roughness; for used values it can be neglected. The check of the validity of this simplification, however, should always be performed.

Measurements of the diffusely scattered intensity can be used for investigating the statistical properties of rough interfaces. Numerical analysis not shown here demonstrated that a fitting procedure for three free parameters (σ_1, Λ_1, and h) cannot be successful since these parameters are correlated if we fit the experimental and the theoretical curves near the Yoneda peaks. Thus, it is more hopeful to determine the rms roughnesses σ_j from the coherent reflectivity measurement and Λ_1 and h from

the Yoneda peaks keeping σ_j fixed. The Λ's of deeper interfaces cannot be determined until the layers are very thin.

The fractal nature of the interfaces is represented by the parameter h. Its determination is complicated by the circumstance that θ_1 scans are most sensitive to h near $\theta_1 \approx \theta_2$, where the form of the experimental scans is distorted by the specular peak. Therefore, h could be stated more precisely from the diffuse scattering measurement if the width of the coherent peak in the experimental θ_1 scan is as small as possible, i.e., one needs a perfectly collimated primary beam with angular divergence under 10 arc sec and a multiple crystal arrangement as an angularly sensitive element instead of a detector slit.

In our theory we have assumed that the rough interfaces are not correlated so that the random functions $u_j(x, y)$ and $u_l(x, y)$ are statistically independent if $j \neq l$. This assumption could be fulfilled for thicker layers. For the case of thinner layers a certain degree of correlation could occur. The influence of that correlation to the diffusely scattered intensity will be the subject of our further investigation.

V. CONCLUSIONS

We have applied the approach of the distorted-wave Born approximation for calculating specular and nonspecular x-ray reflectivity of rough multilayers. We have demonstrated that the angular distribution of the diffusely reflected wave depends not only on basic roughness parameters (rms roughness σ and lateral correlation length Λ) but also on the type of the roughness profile characterized by the fractal dimension $3 - h$. The correspondence of h with the actual surface structure and its preparation technology requires further investigations. We have discussed the possibility of finding all these parameters from reflectivity measurement.

It is well known that the diffusely reflected wave exhibits a maximum if the incidence angle and/or the exit angle equal the critical angle of total reflection (the Yoneda peaks), or if these angles coincide with positions of specular reflectivity maxima of a layered system. The

TABLE III. The geometrical parameters of the experimental arrangement.

	Sample A	Sample B
primary beam width	0.2 mm	0.1 mm
primary beam height	5.0 mm	3.0 mm
detector aperture width	0.5 mm	0.5 mm
detector aperture height	9.0 mm	10.0 mm
sample-detector distance	64 mm	290 mm

above theory explains this fact.

The coincidence of the theory with measurements of the intensity diffusely reflected from metallic layers was quite good. The discrepancy between the theory (if the fractal dimension 2 has been assumed) and experimental results in the case of silicon layers indicates the possibility of investigating the fractal nature of rough interface by means of x-ray reflection.

[1] G. Parrat, Phys. Rev. **95**, 359 (1964).

[2] D. E. Savage, J. Kleiner, N. Schimke, Y.-H. Phang, T. Jankowski, J. Jacobs, R. Kariotis, and M. G. Lagally, J. Appl. Phys. **69**, 1411 (1991).

[3] D. E. Savage, N. Schimke, Y.-H. Phang, and M. G. Lagally, J. Appl. Phys. **71**, 3283 (1992).

[4] D. K. G. de Boer, Phys. Rev. B **44**, 489 (1991).

[5] L. Nevot and P. Croce, Rev. Phys. Appl. **15**, 761 (1980).

[6] B. Vidal and P. Vincent, Appl. Opt. **23**, 1794 (1984).

[7] B. Pardo, T. Megademini, and J. M. André, Rev. Phys. Appl. **23**, 1579 (1988).

[8] Y. Yoneda, Phys. Rev. **131**, 2010 (1963).

[9] O. J. Guentert, J. Appl. Phys. **30**, 1361 (1965).

[10] A. N. Nigam, Phys. Rev. A **4**, 1189 (1965).

[11] J. B. Kortright, J. Appl. Phys. **70**, 3620 (1991).

[12] S. K. Sinha, E. B. Sirota, S. Garoff, and H. B. Stanley, Phys. Rev. B **38**, 2297 (1988).

[13] R. G. Newton, *Scattering Theory of Waves and Particles* (McGraw-Hill, New York, 1966).

[14] H. S. W. Massey, Rev. Mod. Phys. **28**, 199 (1956).

[15] M. K. Sanyal, S. K. Sinha, K. G. Huang, and B. M. Ocko, Phys. Rev. Lett. **66**, 628 (1991); I. M. Tidswell, T. A. Rabedeau, P. S. Pershan, and S. D. Kosowsky, *ibid.* **66**, 2108 (1991).

[16] B. B. Mandelbrodt, *The Fractal Geometry of Nature* (Freeman, New York, 1982), and citations therein.